Original Article

Magnetic resonance imaging features and diagnostic value analysis of non-mass enhancement lesions of the breast

Weiyue Li[1#^], Shaofu Hong[2#^], Yan Shi[1], Jinsen Zou[1], Jie Ma[1^], Jingshan Gong[1]

[1]Department of Radiology, Shenzhen People's Hospital (The Second Clinical Medical College, Jinan University; The First Affiliated Hospital, Southern University of Science and Technology), Shenzhen, China; [2]Department of Ultrasound, Shenzhen People's Hospital (The Second Clinical Medical College, Jinan University; The First Affiliated Hospital, Southern University of Science and Technology), Shenzhen, China

Contributions: (I) Conception and design: W Li, S Hong, J Ma; (II) Administrative support: J Gong, J Ma; (III) Provision of study materials or patients: W Li, Y Shi; (IV) Collection and assembly of data: Y Shi, J Zou; (V) Data analysis and interpretation: W Li, S Hong, Y Shi; (VI) Manuscript writing: All authors; (VII) Final approval of manuscript: All authors.

[#]These authors contributed equally to this work as co-first authors.

Correspondence to: Jingshan Gong, MD, PhD; Jie Ma, BM. Department of Radiology, Shenzhen People's Hospital (The Second Clinical Medical College, Jinan University; The First Affiliated Hospital, Southern University of Science and Technology), No. 1017, Dongmen North Road, Shenzhen 518020, China. Email: jshgong@sina.com; cjr.majie@vip.163.com.

Background: Due to the presence of distinctive morphological features and diverse pathological types, evaluation of breast non-mass enhancement (NME) lesions on magnetic resonance imaging (MRI) is challenging, generating more false-positive results as compared to enhancing mass lesions. Our objective was to identify the MRI features capable of distinguishing between benign and malignant NME lesions in the breast.

Methods: A retrospective analysis was conducted, in which the clinical data and MRI manifestations of 101 NME lesions were examined and confirmed through surgical or biopsy pathology. Statistical analyses, including *t* tests, Wilcoxon rank-sum tests, χ^2 tests, Fisher exact tests, and receiver operating characteristic (ROC) curve analyses, were employed to compare the MRI characteristics and clinical features of benign and malignant NME lesions.

Results: The study included 101 NME lesions from 98 patients (34 benign and 67 malignant). No statistically significant differences were observed in terms of clinical characteristics between the benign and malignant groups. However, there were significant differences in lesion maximum diameter (P=0.003), morphological distribution (P=0.003), internal enhancement patterns (P<0.001), time-intensity curve (TIC) types (P<0.001), early and delayed enhancement rates (P=0.001 and P<0.001, respectively), apparent diffusion coefficient (ADC), and T2 ratio (P=0.02). Notably, the diagnostic efficacy of ADC values was highest for the minimum value within a small region of interest (small ROI), yielding an area under the curve as high as 0.884.

Conclusions: A comprehensive analysis of MRI features indicated their significant value for the differential diagnosis of benign and malignant NME lesions of the breast.

Keywords: Breast; magnetic resonance imaging (MRI); non-mass enhancement (NME); differential diagnosis

Submitted Feb 06, 2024. Accepted for publication Jan 08, 2025. Published online Feb 26, 2025.
doi: 10.21037/qims-24-254
View this article at: https://dx.doi.org/10.21037/qims-24-254

^ ORCID: Weiyue Li, 0009-0004-0974-3254; Shaofu Hong, 0000-0003-3761-6653; Jie Ma, 0000-0003-0648-9786.

Introduction

According to the fifth edition of the American College of Radiology (ACR) Breast Imaging Reporting and Data System (BI-RADS) Atlas (1), breast non-mass enhancement (NME) lesions are defined as areas of enhancing abnormality that do not have a significant mass effect, may be interspersed by normal fibroglandular tissue (FGT) or adipose tissue, and do not have well-defined borders or three-dimensional structures. Although the incidence of NME is low (about 13%) in the general population (2), for clinical practice, it is nonetheless important to identify breast NME because of the wide range of pathological findings. This is because not only do certain ductal carcinoma in situ (DCIS) and nonpalpable invasive cancers manifest as NME so do benign entities (e.g., fibrocystic changes, radiation effects, inflammation, postsurgical scars, hormonal changes, or high-risk lesions such as atypical ductal hyperplasia) (3-5). Therefore, NME has limited value for breast imaging examinations.

Among current breast imaging techniques, magnetic resonance imaging (MRI) boasts high sensitivity for detecting breast lesions (6-8); however, its specificity varies greatly, especially in NME lesions. The lack of typical MRI features in these lesions results in up to 63% of NME lesions being classified as either suspicious or highly suspicious for malignancy (9,10). Therefore, for determining the benign or malignant nature of NME lesions, preoperative core-needle breast biopsy (CNBB) is still required. As a minimally invasive procedure, breast fine needle aspiration biopsy is relatively safe, but there persist potential risks of bleeding, infection, and even dissemination of cancer cells (11,12). With the growth in population undergoing breast-related physical examinations, an increasing number of studies are indicating the potential for breast MRI as a valuable screening method for a broader population of females (13-15). In addition to this, the clinically detectable number of NME lesions is also on the rise. To minimize unnecessary breast biopsies for benign lesions, the capacity to determine the malignant status of NME lesions on MRI urgently needs to be improved. To this end, a greater amount data on MRI differentiation between benign and malignant NME lesions is required.

This study thus aimed to assess the MRI features and diagnostic value of breast NME lesions and provide radiological evidence to facilitate the accurate formulation of clinical diagnostic and therapeutic strategies. We present this article in accordance with the STROBE reporting checklist (available at https://qims.amegroups.com/article/view/10.21037/qims-24-254/rc).

Methods

Patients

This study was conducted in accordance with the Declaration of Helsinki (as revised in 2013) and was approved by ethics board of Shenzhen People's Hospital (No. LL-KY-2022456). The requirement for individual consent was waived due to the retrospective nature of the analysis. A retrospective analysis was conducted on patients who underwent breast MRI examinations at Shenzhen People's Hospital from January 2021 to December 2022. The inclusion criteria were as follows: breast dynamic contrast-enhanced MRI (DCE-MRI) indicating NME; no prior surgery; no history of biopsy, radiotherapy, or chemotherapy before the MRI examination; and no missing pathological data. Meanwhile, the exclusion criteria included poor image quality that rendered parameter measurements unfeasible, coexisting malignant tumors in other systems, and lesions too small for regions of interest to be selected. Ultimately, 98 patients were included, with the data from 101 lesions being analyzed. The patients' ages ranged from 26 to 71 years, with a mean age of 46.52±10.08 years.

Equipment and parameters

A Skyra 3.0T MRI system (Siemens Healthineers, Erlangen, Germany) and a dedicated breast coil were used. Patients were positioned in the prone orientation. The scanning protocols were as follows: (I) axial turbo inversion recovery magnitude (TIRM) sequence [repetition time (TR) =5,000 ms, echo time (TE) =61 ms, slice thickness =4.0 mm, and slice interval =0.8 mm]; and (II) diffusion-weighted imaging (DWI) with a single-shot echo-planar imaging (EPI) sequence (TR =5,700 ms; TE =59 ms; slice thickness =4.0 mm; slice interval =0.8 mm; and b values =50, 400, and 800 s/mm^2) and apparent diffusion coefficient (ADC) maps being automatically generated postreconstruction; and (III) dynamic contrast-enhanced MRI with a 3D spoiled gradient echo fast low-angle shot (FLASH) sequence. A precontrast scan was acquired, followed by a 30-second pause. Subsequently, a bolus injection of contrast agent [gadolinium-diethylenetriamine pentaacetic acid (Gd-DTPA; 2 mL/s, 0.1 mmol/kg)] was injected via the cubital vein, followed by 5 consecutive scans, with a total scan time of 5 minutes 33 seconds.

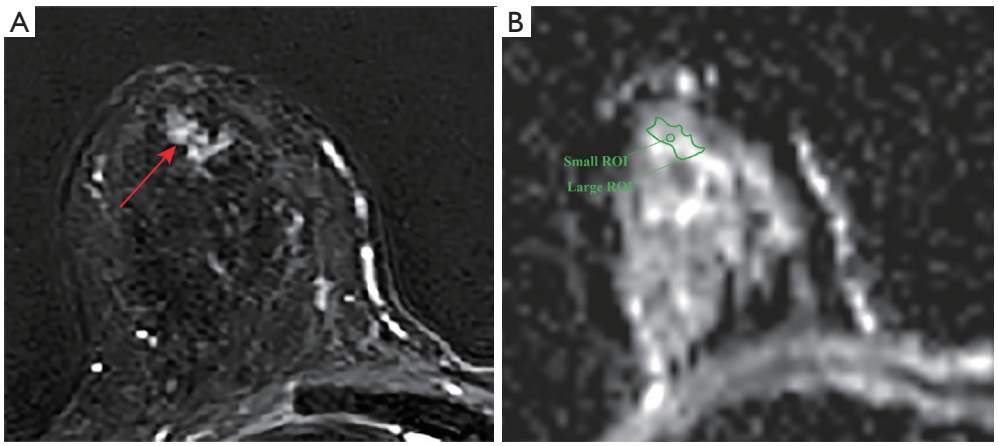

Figure 1 A 49-year-old woman with breast adenosis. (A) A contrast-enhanced subtracted image displaying a lesion with focal and heterogeneous enhancement (arrow). (B) ADC values in this slice were measured using a small ROI and a large ROI on the ADC map. ADC, apparent diffusion coefficient; ROI, region of interest.

Imaging analysis and data measurement method

Two radiologists with >5 years of experience in breast imaging independently reviewed the MRI scans in the absence of clinical and pathological information. They analyzed and documented the results separately, and quantitative data were averaged between the two. In cases of qualitative data disparity, consensus was reached through discussion, and the agreed-upon results were considered for subsequent analyses.

According to the 2013 ACR BI-RADS method (1), maximum diameter, and time-intensity curve (TIC), the distribution and internal enhancement characteristics of NME lesions were recorded and observed. The most significantly enhanced region of the lesion inclusion of normal breast tissue was selected as the region of interest (ROI), with vessels and necrotic, cystic, and hemorrhagic areas being avoided and the inclusion of breast tissue minimized. The early enhancement rate was measured as follows: early enhancement rate = $(SI_2 - SI_0)/SI_0 \times 100\%$, where SI_0 is the precontrast ROI signal intensity, and SI_2 is the postcontrast second-phase ROI signal intensity. Meanwhile, the late enhancement rate was measured as follows: late enhancement rate = $(SI_5 - SI_2)/SI_2 \times 100\%$, where SI_5 is the postcontrast fifth-phase ROI signal intensity. Measurements were performed three times, and the average value was recorded.

Two distinct ROI placement approaches were employed for ADC value measurement: (I) a manually drawn ROI encompassing the visually assessed region with the lowest ADC values within the lesion (small ROI) and (II) an ROI encompassing the entire lesion on the slice with the most obvious enhancement and relatively large lesion section (large ROI) (*Figures 1*,*2*). The minimum ADC value (ADCmin), mean ADC value (ADCmean), and maximum ADC value (ADCmax) were determined. Measurements were performed three times, and the average value was recorded. The TIRM sequence signal ratio of the lesion to the pectoralis major muscle (T2 ratio) was defined as follows: according to the most obvious lesion enhancement on DCE-MRI, the ROI was selected on the TIRM sequence to obtain the lesion signal value and the signal ratio between the lesion and pectoral major muscle at the same slice. Measurements were performed three times, and the average value was recorded. Finally, analysis of the edema surrounding each lesion and the entire ipsilateral breast was performed.

Statistical analysis

Statistical analyses were performed using SPSS 18.0 (IBM Corp. Armonk, NY, USA). Quantitative data are presented as the mean ± standard deviation. Group differences were compared using an independent samples *t* test (for normally distributed data) or the Wilcoxon rank-sum test (for skewed distributions). Qualitative data are expressed as sample size (percentage), and group differences were evaluated using the χ^2 test. The Fisher exact test was used when the

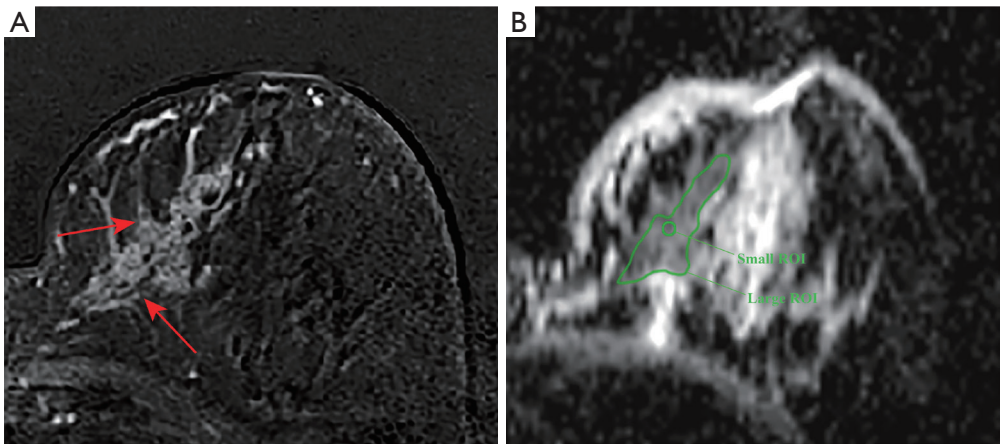

Figure 2 A 56-year-old woman with invasive ductal carcinoma. (A) Contrast-enhanced subtracted image displaying a lesion with segmental and clustered ring enhancement (arrows). (B) ADC values in this slice were measured using a small ROI and a large ROI on the ADC map. ADC, apparent diffusion coefficient; ROI, region of interest.

Table 1 Histopathological category of breast NME lesions

Pathological type	n (%)
Benign (n=34)	
Adenosis	24 (70.6)
Intraductal papilloma	4 (11.8)
Sclerosing adenosis	3 (8.8)
Fibroadenoma	1 (2.9)
Fibrocystic mastopathy	1 (2.9)
Inflammation	1 (2.9)
Malignant (n=67)	
IDC	37 (55.2)
DCIS	22 (32.8)
ILC	4 (6.0)
LCIS	2 (3.0)
Mucinous carcinoma	1 (1.5)
Papillary carcinoma	1 (1.5)

NME, non-mass enhancement; IDC, invasive ductal carcinoma; DCIS, ductal carcinoma *in situ*; ILC, invasive lobular carcinoma; LCIS, lobular carcinoma *in situ*.

expected frequency did not meet the requirements. Receiver operating characteristic (ROC) curve analysis was used to determine the area under the curve (AUC) for ADC values. P<0.05 was considered statistically significant.

Results

Pathological manifestations

This study enrolled 98 patients comprising 101 lesions, 34 (33.7%) of which were benign lesions and 67 (66.3%) malignant. The detailed pathological results are provided in *Table 1*. In our study, multiple sampling was performed on the NME lesions to ensure comprehensive evaluation during biopsy, primarily via the CNBB technique.

Clinical manifestations

There was no significant difference in age between the benign group (45.00±9.2 years) and the malignant group (47.30±10.4 years) (P=0.28). In the benign group, 6 patients (17.6%) were menopausal, while in the malignant group, 24 patients (35.8%) were menopausal, which did not represent a significant difference (P=0.06). Regarding family history, 3 (8.8%) patients in the benign group and 12 (17.9%) patients in the malignant group had a family history of malignancy, but this also did not represent a statistically significant difference (P=0.36).

MRI features

The comparison of MRI features is detailed in *Table 2*. The benign group exhibited a smaller maximum diameter (P=0.003) and a higher prevalence of focal distribution

Table 2 MRI features of breast NME lesions

Characteristic	Benign (n=34)	Malignant (n=67)	P value
Maximum diameter (mm)	30.21±12.04	43.04±20.40	0.003
Distribution			0.003
Focal	13 (38.2)	8 (11.9)	0.002
Linear	3 (8.8)	4 (6.0)	0.594
Segmental	4 (11.8)	35 (52.2)	<0.001
Reginal	6 (17.6)	10 (14.9)	0.723
Multiple regional	4 (11.8)	5 (7.5)	0.473
Diffuse	4 (11.8)	5 (7.5)	0.473
Peritumoral edema			0.019
Present	8 (23.5)	32 (47.8)	
Absent	26 (76.5)	35 (52.2)	
T2 ratio	3.82±1.86	4.46±1.80	0.024
Internal enhancement pattern			<0.001
Homogeneous	15 (44.1)	2 (3.0)	<0.001
Heterogeneous	17 (50.0)	24 (35.8)	0.170
Clumped	0 (0)	19 (28.4)	0.003
Clustered ring	2 (5.9)	22 (32.8)	0.001
TIC			<0.001
Type I	26 (76.5)	7 (10.4)	<0.001
Type II	8 (23.5)	50 (74.6)	<0.001
Type III	0 (0)	10 (14.9)	<0.001
Early enhancement rate (%)	151.28±65.73	193.60±56.11	0.001
Late enhancement rate (%)	15.96±9.23	−0.08±8.39	<0.001

The value of maximum diameter, T2 ratio, and early and late enhancement rate are presented as the mean ± SD, and that of other parameters are presented as no. (%). MRI, magnetic resonance imaging; NME, non-mass enhancement; TIC, time-intensity curve; SD, standard deviation.

(38.2%; P=0.002) compared to the malignant group, which primarily demonstrated segmental distribution (52.2%; P<0.001) (*Figures 1*,*2*) and had a greater proportion of cases with peritumoral edema (P=0.02) (*Figure 3*). The benign group mostly showed heterogeneous and homogeneous internal enhancement patterns, while the malignant group rarely displayed homogeneous patterns. Beyond heterogeneous enhancement, significant differences were observed for the other three enhancement patterns (*Figure 4*). Regarding TIC types, type I predominated in the benign group, with types II and III being more common in the malignant group (P<0.001) (*Figure 5*). Additionally, the benign group showed lower early enhancement rates (P=0.001) and higher late enhancement rates (P<0.001). As shown in *Table 3* and *Figure 6*, for small ROIs, the benign group's ADCmin, ADCmean, and ADCmax were significantly higher than those of the malignant group (P<0.001). For large ROIs, the benign group's ADCmin and ADCmean were significantly higher than those of the malignant group (P<0.05). Among these, ADCmin with small ROIs had the highest AUC (0.884). Concerning the T2 ratio, the malignant group had a significantly higher ratio than did the benign group (P=0.02). However, when cases with peritumoral edema were excluded, the T2 ratio was 3.97±2.01 for the benign group and 4.44±2.17 for the malignant group, which did not represent a statistically significant difference (P=0.39).

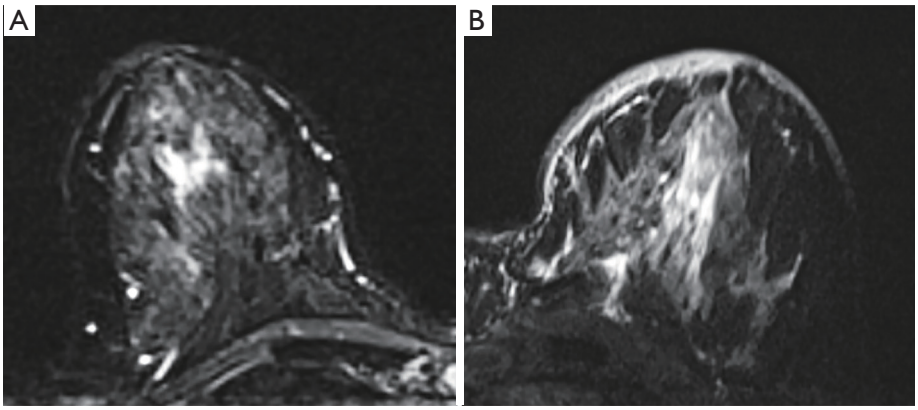

Figure 3 TIRM images. (A) No significant edema surrounding the lesion in the right breast with breast adenosis (same patient as in *Figure 1*). (B) Peritumoral edema and subcutaneous edema around the left breast invasive ductal carcinoma lesion (same patient as in *Figure 2*). TIRM, turbo inversion recovery magnitude sequence.

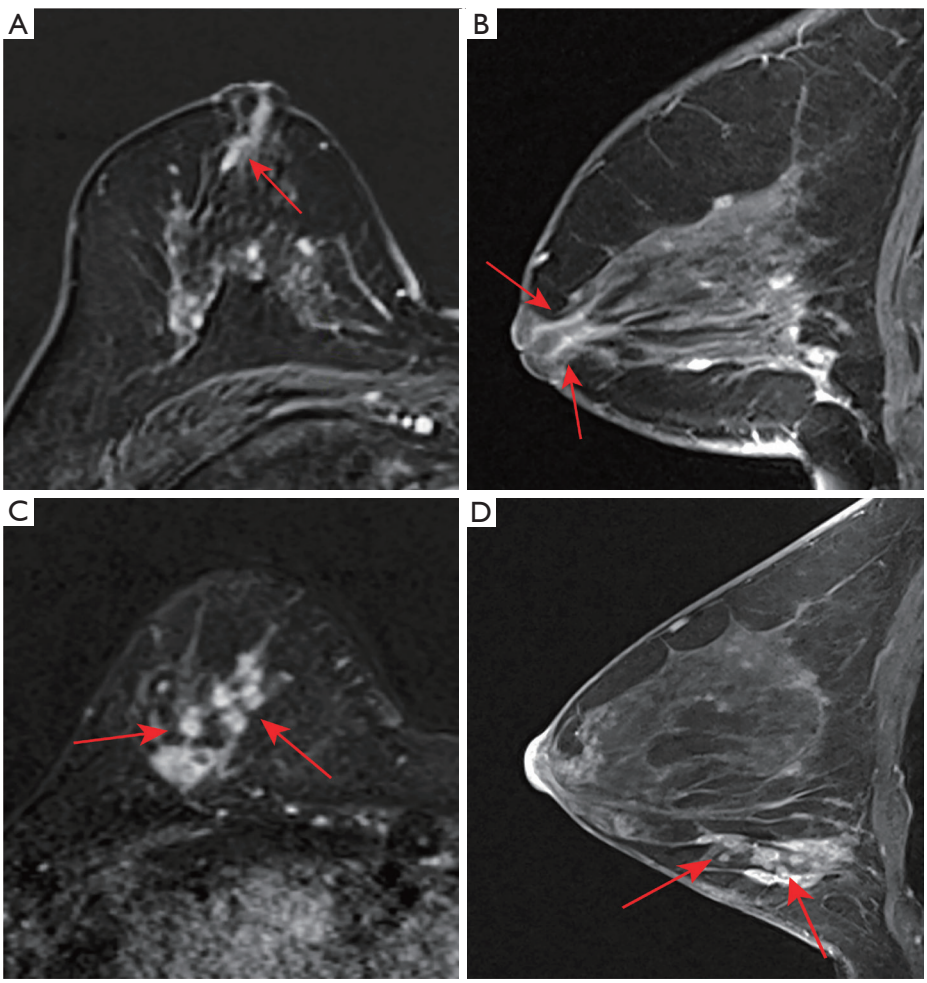

Figure 4 Contrast-enhanced image. (A) Axial and (B) sagittal views showing a linear, homogeneous enhancing lesion (arrows) in the right breast of a 60-year-old female patient with intraductal papilloma, accompanied by adjacent ductal dilatation. (C) Axial and (D) sagittal views showing segmental and clustered enhancing lesions (arrows) in the right breast of a 35-year-old female patient with invasive ductal carcinoma.

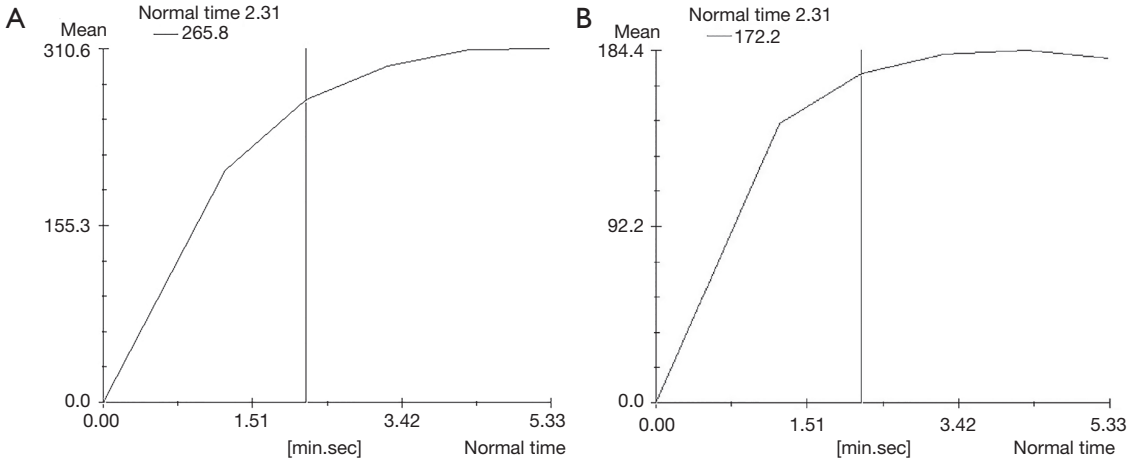

Figure 5 TIC showing (A) a type I curve for breast adenosis (same patient as in *Figure 1*) and (B) a type II curve for breast invasive ductal carcinoma (same patient as in *Figure 2*). The Y-axis represents the difference between the signal intensity of the NME lesion on DCE-MRI and the precontrast signal intensity. TIC, time-intensity curve; DCE-MRI, dynamic contrast-enhanced magnetic resonance imaging; NME, non-mass enhancement.

Table 3 ADC values (mm^2/s) and AUCs for different ROIs

Variable	Benign	Malignant	P value	AUC
Small ROI				
ADCmin	1,201.23±193.86	882.52±197.65	<0.001	0.884
ADCmean	1,314.09±211.04	1,021.37±216.22	<0.001	0.832
ADCmax	1,433.82±259.22	1,186.51±280.45	<0.001	0.755
Large ROI				
ADCmin	828.61±226.63	711.32±172.71	0.013	0.672
ADCmean	1258.13±259.96	1150.53±217.18	0.041	0.615
ADCmax	1771.39±367.91	1705.85±347.63	0.391	0.578

The values of ADC are presented as the mean ± SD. ADC, apparent diffusion coefficient; AUC, area under the curve; ROI, region of interest; ADCmin, the minimum apparent diffusion coefficient; ADCmean, the mean apparent diffusion coefficient; ADCmax, the maximum apparent diffusion coefficient; SD, standard deviation.

Discussion

Due to the particular manifestations of breast NME lesions, determining benignancy and malignancy from MRI can be challenging. Therefore, the aim of this study was to examine the MRI characteristics of breast NME and analyze the differences between benign and malignant cases.

In terms of morphological distribution, our study revealed that malignant breast NME lesions often exhibited a significantly higher proportion of segmental distribution (52.2%) as compared to benign lesions (11.8%) (P<0.001), which is consistent with previous studies (2,16,17). This is likely due to the predominance of ductal carcinoma (88.1%) in our malignant cases, which typically presents with a segmental distribution along ductal bundles, forming a distinctive anatomical pattern (18,19). In contrast, among the 34 benign cases in our group, 13 (38.2%) demonstrated focal distribution (*Table 2*), a proportion significantly higher than that of malignant lesions (11.9%) (P=0.002), which is consistent with previous studies (17,20). However, some research (18,21) has reported significant differences in the linear distribution between benign and malignant lesions. This could be attributed to variations in the proportion of pathological types, as seen in the study by Liu *et al.* (21),

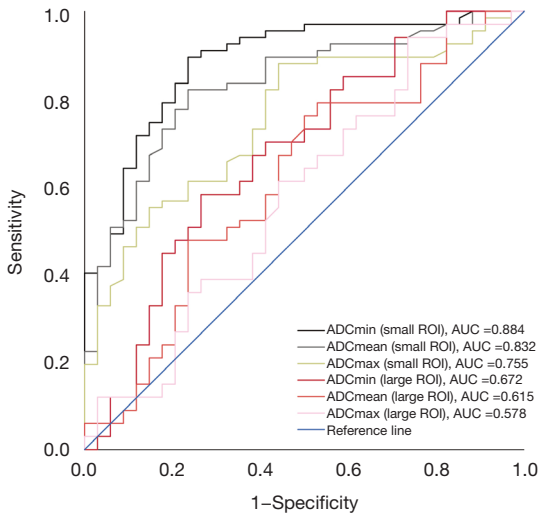

Figure 6 ROC curves and AUC for the minimum, mean, and maximum ADC of small ROIs and large ROIs. ROC, receiver operating characteristic; AUC, area under the curve; ROI, region of interest; ADC, apparent diffusion coefficient; ADCmin, the minimum apparent diffusion coefficient; ADCmean, the mean apparent diffusion coefficient; ADCmax, the maximum apparent diffusion coefficient.

where benign cases primarily comprised intraductal papilloma (38.7%) and inflammation (25.8%); whereas, 70.6% of our cohort consisted of adenosis. Another contributing factor is the limited number of benign cases included in our study. Thus, further investigations with larger sample sizes that examine different pathological subtypes of benign breast NME lesions are warranted to elucidate these differences. Additionally, the measurement of the maximum diameter in our cohort involved joint assessment in both the axial and sagittal slices, with the maximum length being selected as the lesion's long axis. The maximum diameter of benign lesions in our study often corresponded to a focal or regional extension, differing from the malignancies in which the maximum diameter followed the course of the ducts. Consequently, benign NME lesions exhibited a significantly smaller maximum diameter.

Multiple studies (16,18,20) have indicated that clustered ring enhancement is the predominant internal enhancement feature of malignant breast NME lesions. Similar findings were observed in our cohort, with the frequency of clustered ring enhancement in malignant lesions (32.8%) being significantly higher than that in benign ones (P=0.001). The pathological basis for this manifestation is primarily the propensity of malignant lesions to undergo necrotic and cystic changes: the degree of enhancement within the tumor area decreases as contrast agent washes out following early enhancement, while the persistent enhancement of ductal walls and surrounding stroma have rich vascularity (16,20,22). We also found that lesions with clumped enhancement demonstrated a significantly correlation with malignancy (P=0.003), which is consistent with previous studies (16,17). This suggests that clustered ring and clumped enhancement have a relatively reliable diagnostic value for identifying malignant lesions.

However, the proportion of homogeneously enhanced benign NME lesions (44.1%) was noticeably higher than that of malignant lesions (P<0.001), which contrasts with the studies by Liu *et al.* (21) and Aydin (18). The pathological composition and the limited number of benign cases may be contributing factors, and further validation with a larger sample size is warranted. From *Table 2*, it can be observed that two cases of benign NME lesions (adenosis) exhibited clumped ring enhancement. Analysis of the T2-weighted imaging sequences in these two cases revealed multiple small cystic changes within the lesions. Therefore, in benign lesions, the presence of clumped ring enhancement may be correlated with small cystic changes. However, in both benign and malignant groups, the most prevalent internal enhancement pattern was heterogeneous enhancement, indicating substantial overlap in enhancement features. This underscores the challenge of assessing NME in terms of enhancement patterns, and experienced readers should comprehensively consider multiple imaging features of MRI.

In this study, the most common TIC for malignant lesions was type II (74.6%), which is consistent with the findings reported by Aydin (18) and Liu *et al.* (17). Although only 10 out of 67 (14.9%) malignant lesions exhibited type III curves, this difference remained statistically significant as compared to benign lesions. Benign lesions were predominantly characterized by type I curves (76.5%). Compared to benign lesions, malignant lesions exhibited a higher early enhancement rate (P=0.001) and a significantly reduced late enhancement rate (P<0.001). Hence, TIC and enhancement rates can be considered valuable indicators of malignancy in breast NME lesions (23). This may be due to the prominent vascularization within malignant lesions, characterized by increased neoangiogenesis and enhanced permeability, resulting in faster contrast agent washout (24). However, the application of TIC and enhancement rates relies on the selection of the ROI. Given the marked

internal morphological heterogeneity of breast NME lesions, which may cause partial volume effects and affect result stability, a comprehensive consideration of lesion morphology distribution, internal enhancement patterns, and other factors is still required.

In our study, the T2 signal ratio between malignant breast NME lesions and the chest muscle was significantly higher than that of benign lesions in TIRM sequences. However, an intriguing observation from our study was the statistically significant association between peritumoral edema and lesion malignancy. When cases with peritumoral edema were excluded, a significant difference in the T2 signal ratio between benign and malignant lesions was not observed. This suggests that the elevated T2-weighted imaging signal in malignant lesions may primarily be attributed to peritumoral edema. The invasive growth of malignant lesions is linked to increased proteolytic activity in the peritumoral region and neovascularization. The latter contributes to heightened vascular permeability, leading to increased fluid extravasation around the vessels and subsequent peritumoral edema (24-26). Therefore, the presence of peritumoral edema on TIRM sequences may serve as an marker for malignancy in breast NME lesions.

DWI, a method for assessing tissue diffusion rates, provides information on tissue microstructure and cell density, with ADC being its quantitative index (8). Previous studies (17,21) predominantly employed a single ADC value and a single ROI for evaluation, and some studies (10,27) even suggested that a single ADC value can provide limited additional value to DCE-MRI in NME assessment. However, due to the lack of well-defined three-dimensional structures in breast NME lesions, both benign and malignant lesions may contain interspersed normal tissues, leading to pronounced internal morphological heterogeneity (28). This heterogeneity causes the MRI features of benign and malignant lesions to overlap, posing a significant challenge to qualitative diagnostic analysis. Therefore, in our study, ADCmin, ADCmean, and ADCmax from different ROIs were used. The results indicated that the ADC values of breast NME lesions were significantly influenced by the size of the ROI, with ADCmin, ADCmean, and ADCmax of malignant lesions in small ROIs being markedly lower than those of benign lesions. Particularly, ADCmin exhibited the highest diagnostic efficacy, with the reduction in ADCmin values of malignant lesions relative to ADCmean and ADCmax being greater than that of benign lesions. This can be explained primarily by the significant internal structural heterogeneity of the benign and malignant breast NME lesions leading to inadvertent inclusion of normal breast tissue or necrotic cystic areas during ROI delineation and thereby affecting the ADCmean and ADCmax. However, ADCmin can represent the most cellularly dense region within the lesion, which is highly relevant to tumor malignancy and serves as the key differentiating feature between benign and malignant tumor lesions, thus contributing to higher diagnostic accuracy (27,29).

Although theoretically, a large ROI covering the whole lesion could encompass tumor regions with the lowest ADC values, our results showed that its diagnostic efficacy is relatively lower. The lower AUC value might be attributed to (I) susceptibility to volume effects due to edges or gaps in tumor tissue within large ROIs leading to potential miscalculation in fat-suppressed regions (27,28); (II) morphological variability of NME lesions causing different observers to report inconsistent ranges for large ROIs, thus generating unstable results; and (III) a certain degree of inherent spatial distortions observed in most DWI sequences (30) potentially causing lesions within large ROIs to not be entirely representative of the most enhanced or densely populated areas of tumor cells, thereby confounding the calculation results. Therefore, in the differentiation of benign and malignant breast NME lesion, the use of small ROI ADCmin values can help mitigate the subjectivity of radiologists' interpretations and avoid misdiagnosis due to limited experience.

Certain limitations to this study should be noted: (I) first, we employed a retrospective design, and cases with pathology underwent mostly symptomatic or secondary examinations, which could have led to a higher proportion of malignant NME lesions. Future studies should target screening populations for more balanced results. (II) There was potential interobserver variability in the observational parameters, necessitating further assessment in subsequent studies. (III) Finally, the sample size was limited, and additional data collection is required to validate the results.

Conclusions

According to our findings, benign breast NME lesions exhibit focal distribution, homogeneous internal enhancement, and type I kinetics, while malignant lesions often present with segmental distribution or clustered ring or clumped enhancement with type II or III kinetics and are more prone to peritumoral edema. The ADCmin value from small ROIs demonstrated higher diagnostic efficacy in

the qualitative assessment of breast NME lesions. Through the analysis and summary of MRI features of breast NME lesions, we aim to provide robust imaging evidence for clinical decision-making and reduce unnecessary breast biopsies.

Acknowledgments

None.

Footnote

Reporting Checklist: The authors have completed the STROBE reporting checklist. Available at https://qims.amegroups.com/article/view/10.21037/qims-24-254/rc

Funding: This work was supported by the Shenzhen Science and Technology Research and Development Fund (No. GJHZ20210705142208024) and the Shenzhen Science and Technology Research and Development Fund (No. GJHZ20220913142613025).

Conflicts of Interest: All authors have completed the ICMJE uniform disclosure form (available at https://qims.amegroups.com/article/view/10.21037/qims-24-254/coif). J.G. serves as an unpaid editorial board member of *Quantitative Imaging in Medicine and Surgery*. The other authors have no conflicts of interest to declare.

Ethical Statement: The authors are accountable for all aspects of the work in ensuring that questions related to the accuracy or integrity of any part of the work are appropriately investigated and resolved. This study was conducted in accordance with the Declaration of Helsinki (as revised in 2013) and was approved by ethics board of Shenzhen People's Hospital (No. LL-KY-2022456). The requirement for individual consent was waived due to the retrospective nature of the analysis.

References

1. Morris EA, Comstock CE, Lee CH, Lehman CD, Ikeda DM, Newstead GM, Tozaki M, Hylton N, Helbich TH, Kuhl C, Monticciolo DL, Schnall MD, Wolfman JA. ACR BI-RADS® Magnetic Resonance Imaging. In: ACR BI-RADS® Atlas, Breast Imaging Reporting and Data System. American College of Radiology; 2013.
2. Yang QX, Ji X, Feng LL, Zheng L, Zhou XQ, Wu Q, Chen X. Significant MRI indicators of malignancy for breast non-mass enhancement. J Xray Sci Technol 2017;25:1033-44.
3. Hong S, Li W, Gao W, Liu M, Song D, Dong Y, Xu J, Dong F. Diagnostic performance of elastography for breast non-mass lesions: A systematic review and meta-analysis. Eur J Radiol 2021;144:109991.
4. Manion E, Brock JE, Raza S, Reisenbichler ES. MRI-guided breast needle core biopsies: pathologic features of newly diagnosed malignancies. Breast J 2014;20:453-60.
5. Qu XX, Song Y, Zhang YH, Qing HM. Value of Ultrasonic Elastography and Conventional Ultrasonography in the Differential Diagnosis of Non-Mass-like Breast Lesions. Ultrasound Med Biol 2019;45:1358-66.
6. Mann RM, Cho N, Moy L. Breast MRI: State of the Art. Radiology 2019;292:520-36.
7. Gweon HM, Cho N, Seo M, Chu AJ, Moon WK. Computer-aided evaluation as an adjunct to revised BI-RADS Atlas: improvement in positive predictive value at screening breast MRI. Eur Radiol 2014;24:1800-7.
8. Kubota K, Mori M, Fujioka T, Watanabe K, Ito Y. Magnetic resonance imaging diagnosis of non-mass enhancement of the breast. J Med Ultrason (2001) 2023;50:361-6.
9. Gity M, Ghazi Moghadam K, Jalali AH, Shakiba M. Association of Different MRI BIRADS Descriptors With Malignancy in Non Mass-Like Breast Lesions. Iran Red Crescent Med J 2014;16:e26040.
10. Marino MA, Avendano D, Sevilimedu V, Thakur S, Martinez D, Lo Gullo R, Horvat JV, Helbich TH, Baltzer PAT, Pinker K. Limited value of multiparametric MRI with dynamic contrast-enhanced and diffusion-weighted imaging in non-mass enhancing breast tumors. Eur J Radiol 2022;156:110523.
11. Loving VA, Johnston BS, Reddy DH, Welk LA, Lawther HA, Klein SC, Cranford CM, Reed RC, Rangan P, Morris MF. Antithrombotic Therapy and Hematoma Risk during Image-guided Core-Needle Breast Biopsy. Radiology 2023;306:79-86.
12. Maseki H, Jimbo K, Watase C, Murata T, Shiino S,

Takayama S, Yamamoto N, Satomi K, Maeshima A, Yoshida M, Suto A. Clinical significance of tumor cell seeding associated with needle biopsy in patients with breast cancer. Asian J Surg 2023;46:3700-4.
13. Bakker MF, de Lange SV, Pijnappel RM, Mann RM, Peeters PHM, Monninkhof EM, et al. Supplemental MRI Screening for Women with Extremely Dense Breast Tissue. N Engl J Med 2019;381:2091-102.
14. Kuhl CK, Strobel K, Bieling H, Leutner C, Schild HH, Schrading S. Supplemental Breast MR Imaging Screening of Women with Average Risk of Breast Cancer. Radiology 2017;283:361-70.
15. Monticciolo DL, Newell MS, Moy L, Niell B, Monsees B, Sickles EA. Breast Cancer Screening in Women at Higher-Than-Average Risk: Recommendations From the ACR. J Am Coll Radiol 2018;15:408-14.
16. Asada T, Yamada T, Kanemaki Y, Fujiwara K, Okamoto S, Nakajima Y. Grading system to categorize breast MRI using BI-RADS 5th edition: a statistical study of non-mass enhancement descriptors in terms of probability of malignancy. Jpn J Radiol 2018;36:200-8.
17. Liu D, Ba Z, Gao Y, Wang L. Subcategorization of suspicious non-mass-like enhancement lesions(BI-RADS-MRI Category4). BMC Med Imaging 2023;23:182.
18. Aydin H. The MRI characteristics of non-mass enhancement lesions of the breast: associations with malignancy. Br J Radiol 2019;92:20180464.
19. Salvatorelli L, Puzzo L, Vecchio GM, Caltabiano R, Virzì V, Magro G. Ductal Carcinoma In Situ of the Breast: An Update with Emphasis on Radiological and Morphological Features as Predictive Prognostic Factors. Cancers (Basel) 2020;12:609.
20. Lunkiewicz M, Forte S, Freiwald B, Singer G, Leo C, Kubik-Huch RA. Interobserver variability and likelihood of malignancy for fifth edition BI-RADS MRI descriptors in non-mass breast lesions. Eur Radiol 2020;30:77-86.
21. Liu G, Li Y, Chen SL, Chen Q. Non-mass enhancement breast lesions: MRI findings and associations with malignancy. Ann Transl Med 2022;10:357.
22. Chadashvili T, Ghosh E, Fein-Zachary V, Mehta TS, Venkataraman S, Dialani V, Slanetz PJ. Nonmass enhancement on breast MRI: review of patterns with radiologic-pathologic correlation and discussion of management. AJR Am J Roentgenol 2015;204:219-27.
23. Soylu Boy FN, Esen Icten G, Kayadibi Y, Tasdelen I, Alver D. Idiopathic Granulomatous Mastitis or Breast Cancer? A Comparative MRI Study in Patients Presenting with Non-Mass Enhancement. Diagnostics (Basel) 2023;13:1475.
24. Santucci D, Faiella E, Cordelli E, Calabrese A, Landi R, de Felice C, Beomonte Zobel B, Grasso RF, Iannello G, Soda P. The Impact of Tumor Edema on T2-Weighted 3T-MRI Invasive Breast Cancer Histological Characterization: A Pilot Radiomics Study. Cancers (Basel) 2021;13:4635.
25. Baltzer PA, Yang F, Dietzel M, Herzog A, Simon A, Vag T, Gajda M, Camara O, Kaiser WA. Sensitivity and specificity of unilateral edema on T2w-TSE sequences in MR-Mammography considering 974 histologically verified lesions. Breast J 2010;16:233-9.
26. Xu Z, Ding Y, Zhao K, Han C, Shi Z, Cui Y, Liu C, Lin H, Pan X, Li P, Chen M, Wang H, Deng X, Liang C, Xie Y, Liu Z. MRI characteristics of breast edema for assessing axillary lymph node burden in early-stage breast cancer: a retrospective bicentric study. Eur Radiol 2022;32:8213-25.
27. Avendano D, Marino MA, Leithner D, Thakur S, Bernard-Davila B, Martinez DF, Helbich TH, Morris EA, Jochelson MS, Baltzer PAT, Clauser P, Kapetas P, Pinker K. Limited role of DWI with apparent diffusion coefficient mapping in breast lesions presenting as non-mass enhancement on dynamic contrast-enhanced MRI. Breast Cancer Res 2019;21:136.
28. Bickel H, Pinker K, Polanec S, Magometschnigg H, Wengert G, Spick C, Bogner W, Bago-Horvath Z, Helbich TH, Baltzer P. Diffusion-weighted imaging of breast lesions: Region-of-interest placement and different ADC parameters influence apparent diffusion coefficient values. Eur Radiol 2017;27:1883-92.
29. Li T, Hong Y, Kong D, Li K. Histogram analysis of diffusion kurtosis imaging based on whole-volume images of breast lesions. J Magn Reson Imaging 2020;51:627-34.
30. Bogner W, Pinker-Domenig K, Bickel H, Chmelik M, Weber M, Helbich TH, Trattnig S, Gruber S. Readout-segmented echo-planar imaging improves the diagnostic performance of diffusion-weighted MR breast examinations at 3.0 T. Radiology 2012;263:64-76.

Cite this article as: Li W, Hong S, Shi Y, Zou J, Ma J, Gong J. Magnetic resonance imaging features and diagnostic value analysis of non-mass enhancement lesions of the breast. Quant Imaging Med Surg 2025;15(3):2457-2467. doi: 10.21037/qims-24-254

